Frontiers of Physics
https://doi.org/10.1007/s11467-021-1131-4
Front. Phys.
17(3), 33504 (2022)

RESEARCH ARTICLE

Thermal control magnetic switching dominated by spin reorientation transition in Mn-doped $PrFeO_3$ single crystals

Wencheng Fan[1], Haiyang Chen[1], Gang Zhao[1], Xiaoxuan Ma[1], Ramki Chakaravarthy[1], Baojuan Kang[1], Wenlai Lu[1,†], Wei Ren[1,2], Jincang Zhang[1,2], Shixun Cao[1,2,‡]

[1] *Materials Genome Institute, Department of Physics and International Center for Quantum and Molecular Structures, Shanghai University, Shanghai 200444, China*
[2] *Shanghai Key Laboratory of High Temperature Superconductors, Shanghai University, Shanghai 200444, China*
Corresponding authors. E-mail: †wenlai@t.shu.edu.cn, ‡sxcao@shu.edu.cn
Received July 17, 2021; accepted November 15, 2021

Spin reorientation transition (SRT) has attracted substantial attention due to its important role in the ultrafast control of spins. However, the transition temperature is usually too low for its practical applications. Here, we demonstrate the ability to modulate the SRT temperature in $PrFe_{1-x}Mn_xO_3$ single crystals from 196 K to 317 K across the room temperature by varying the Mn concentration. Interestingly, the Γ_4 to Γ_1 spin reorientation of the Mn-doped $PrFeO_3$ is distinct from the Γ_4 to Γ_2 spin reorientation transition as in the parent material. Because of the coupling between rare-earth ions and transition-metal ions in determining the SRT temperature, the demonstrated control scheme of spin reorientation transition temperature by Mn-doping is expected to be used in temperature control magnetic switching devices and applicable to many other rare-earth orthoferrites.

Keywords magnetic switching, spin reorientation transition, perovskite oxides

1 Introduction

Antiferromagnetic materials, though representing the overwhelming majority of magnetic materials, were of academic interest only for a long time because of their large rigidity to an external field. Their ultrafast dynamics of spins, which is a key issue for exchange-biased devices [1], expands the limited set of their applications and make them outstanding candidates for future information technologies where magnetization reversal is a basic component [2]. The spin of antiferromagnetic materials can indeed be manipulated on picosecond time scales by photoexcitation of temperature-induced spin reorientation (SR) phase transitions [3], which is the key to achieve comparable operating speeds with charge-based devices [4]. By contrast, in a ferromagnetic medium it is only a few hundred picoseconds [5, 6].

Rare earth orthoferrites [7] $RFeO_3$ (R is a rare-earth element) is a typical class of materials that hosts ultrafast SR phase transitions and crystallizes in an orthorhombically distorted perovskite structure [8]. Below the Néel temperature (T_N = 650–700 K), the Fe^{3+} antiferromagnetic order is formed, but due to the inclination between the magnetic moments formed by the Fe^{3+} spin in $RFeO_3$, the weak ferromagnetic moment is coupled to the initial antiferromagnetic order through the Dzyaloshinskii–Moriya interaction [9]. In $RFeO_3$, the interaction between R-4f and Fe-3d has been found to couple the weak ferromagnetic moment of Fe^{3+} to the rare-earth ions R^{3+}. The competing magnetic anisotropy between R^{3+} and Fe^{3+} will cause spin reorientation in $RFeO_3$ [10].

Up till now, however, the SR transitions occur mostly at low temperatures in rare-earth orthoferrites with the only exception of $SmFeO_3$ [11] exhibiting a SR transition temperature at 450–480 K which is too high for application, limiting their practical applications in the ultrafast regime [10]. Indeed, the reported temperature of ultrafast control of spins is < 90 K for $TmFeO_3$ [3, 12], < 50 K for $HoFeO_3$ [13, 14], < 40 K for $DyFeO_3$ [15]. Therefore, the modulation of SR transition temperature and the realization of the room temperature SR transition in rare-earth orthoferrites would be of great importance for SR-based technologies.

Considering the strong coupling between the R^{3+} and Fe^{3+} in determining the SR transition temperature [10], one strategy to modulate the SR transition temperature is by rare-earth doping and this has been investigated intensively in various orthoferrites [16–22]. In contrast, there has been considerably less investigations of rare-earth or-

* This article can also be found at http://journal.hep.com.cn/fop/EN/10.1007/s11467-021-1131-4.

thoferrites by introducing transition-metal elements at the Fe site. Recently, it has been found that the SR transition appears in oxypnictides and oxides other than orthoferrites due to the strong coupling between magnetic R^{3+} and the transition metal ions such as Mn, Cr and Fe [23, 24]. It is therefore natural to introduce Mn or Cr at the transition-metal site of rare-earth orthoferrites as an alternative to modulate the SR transition temperature.

Here, we choose $PrFeO_3$ [25, 26] as a prototypical orthoferrite to study the SR phase transition by Mn doping. A series of Mn-doped $PrFe_{1-x}Mn_xO_3$ (where $x = 0$, 0.1, 0.2, 0.25, 0.3) single crystals have been grown by optical floating zone method. It has been found that the SR transition temperature is largely dependent on Mn doping and the room temperature SR phase transition has been achieved at the doping level $x = 0.25$. The SR phase transitions of all the Mn-doped $PrFeO_3$ samples are a transition from a noncollinear antiferromagnetic phase Γ_4 with the net moments along the c axis to a collinear compensated antiferromagnetic phase Γ_1 upon cooling. Interestingly, such a transition is drastically different from the second-order transition between two noncollinear antiferromagnetic phases Γ_4 and Γ_2 with the net moments along c and a axes as found in the parent $PrFeO_3$ material. Therefore, $PrFe_{1-x}Mn_xO_3$ can be a new type of magnetic temperature-sensitive material with the effect of thermal-controllable magnetic switching.

2 Experimental method

A series of Mn-doped $PrFe_{1-x}Mn_xO_3$ ($x = 0$, 0.1, 0.2, 0.25, 0.3) powders were prepared by solid state reaction method using the high purity starting materials of Pr_6O_{11} (99.99%), Fe_2O_3 (99.9%) and MnO_2 (99.9%). They were accurately weighed and mixed according to the stoichiometric ratio. After uniform grinding, they were then placed into a high-temperature sintering furnace at 1250 °C and sintered for 1000 minutes to ensure the structural formation. $PrFe_{1-x}Mn_xO_3$ single crystals were then obtained from the synthesized polycrystalline samples by optical floating zone method (FZ-T-10000-H-VI-P-SH, Crystal Systems Corp). During the crystal growth process, the surface tension of the molten zone is smaller owing to the Mn-doping in $PrFe_{1-x}Mn_xO_3$ samples. In order to keep the molten zone stable, a growth rate of 5 mm/h is required, which is faster than that of $PrFeO_3$ single crystals. The upper and lower rods rotate simultaneously in opposite directions at a speed of 15 rpm. X-ray diffraction (XRD, Bruker D2 PHASER) was used to characterize the crystal structure and confirm phase purity and crystal quality. X-ray back reflection Laue crystal diffractometer (Try-SE. Co, Ltd.) was used to determine the crystallographic orientation of all single crystals. Physical property measurement system (PPMS DynaCool-14T) with a vibrating sample magnetometer (VSM) option was used to measure the magnetization under different temperatures and magnetic fields.

3 Results and discussion

3.1 Structure characterization

The Laue diagrams of the $PrFe_{1-x}Mn_xO_3$ ($x = 0$, 0.1, 0.2, 0.25, 0.3) series single crystals along three crystal axes of each single crystal are shown in Fig. 1. The very clear and sharp Laue diffraction spots indicate that the single crystals are of good quality. A piece of the $PrFe_{1-x}Mn_xO_3$ ($x = 0$, 0.1, 0.2, 0.25, 0.3) single crystals has been ground into very fine powder for powder X-ray diffraction and the FullProf software was used to refine the crystal structure data as shown in Figs. 2(a)–(e). It can be inferred from Figs. 2(a)–(e) that the grown samples are of single phase without any impurity peaks and have the same orthorhombic structure with *Pbnm* space group of the parent $PrFeO_3$ phase. That is, the doping of Mn does not alter the crystal structure of the $PrFeO_3$ crystals. The refined lattice constants of $PrFe_{1-x}Mn_xO_3$ are shown in Fig. 2(f). It shows that the lattice constant c of $PrFe_{1-x}Mn_xO_3$ samples decreases whereas the lattice constant b increases with Mn doping.

3.2 Magnetization measurements

The temperature dependent magnetization (M–T) of the $PrFe_{1-x}Mn_xO_3$ single crystals measured in the zero-field-cooled (ZFC) mode under an applied field of 100 Oe along the c-axis was shown in Fig. 3. An abrupt change in magnetization is observed for all the ZFC curves, implying a SR phase transition of all the grown $PrFe_{1-x}Mn_xO_3$ single crystals. Moreover, the SR transition temperature shifts from 194–196 K towards higher temperature at 315–317 K with increasing the Mn doping. That is, the SR transition temperature is successfully controlled in $PrFe_{1-x}Mn_xO_3$ single crystals by the different doping of Mn, and that the

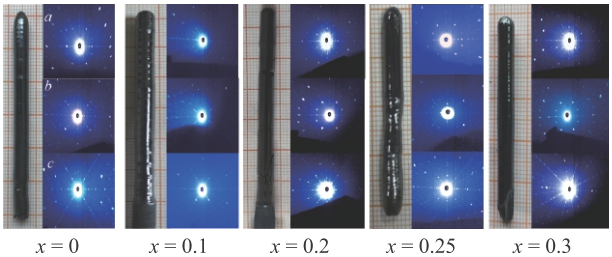

Fig. 1 The morphology and the Laue diffraction patterns along a, b, c axes of $PrFe_{1-x}Mn_xO_3$ ($x = 0$, 0.1, 0.2, 0.25, 0.3) single crystals.

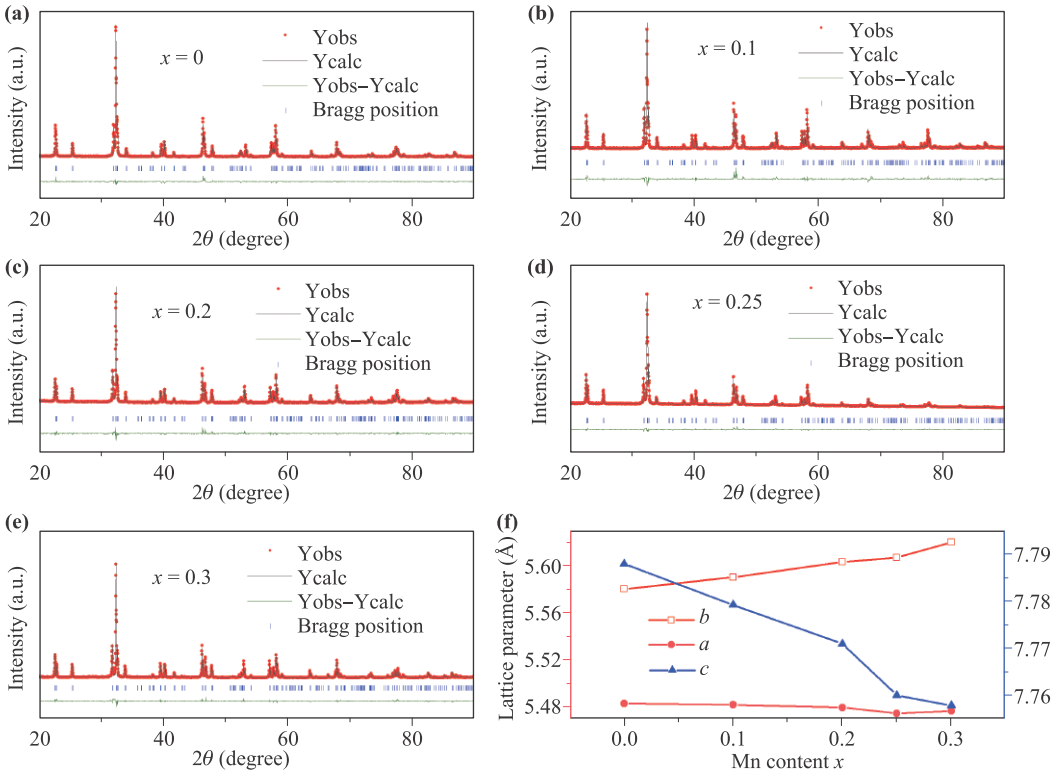

Fig. 2 **(a–e)** The XRD refined structure patterns of $PrFe_{1-x}Mn_xO_3$ (x = 0, 0.1, 0.2, 0.25, 0.3) at room temperature. **(f)** The three lattice constants of a, b and c of $PrFe_{1-x}Mn_xO_3$ with different Mn concentrations.

room temperature SR has indeed realized. It should be noted from Fig. 3 that the transition temperature interval ΔT for all the samples is around 2 K, which is quite sharp. In addition, the magnetization of $PrFe_{1-x}Mn_xO_3$ single crystals above the transition temperature decreases with the increase of Mn doping. One possible reason is that the canted antiferromagnetic structure of Fe is destroyed by the doping of Mn, which weakens the macroscopic magnetization of the system [27–30].

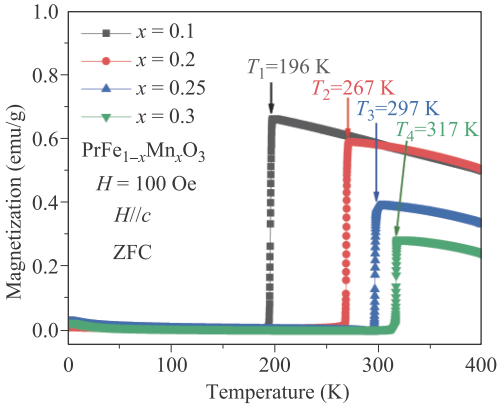

Fig. 3 ZFC curves of $PrFe_{1-x}Mn_xO_3$ single crystals with different doping under an external magnetic field of 100 Oe along the c-axis.

In order to identify the phase transition type of the observed spin reorientation, temperature dependent magnetization measurements were carried out along the a and b axes in addition to the c axis. The measurements of all the Mn-doped $PrFeO_3$ single crystals have similar results. To be concise, we take the $PrFe_{0.75}Mn_{0.25}O_3$ single crystal as a representative here to show the results. The

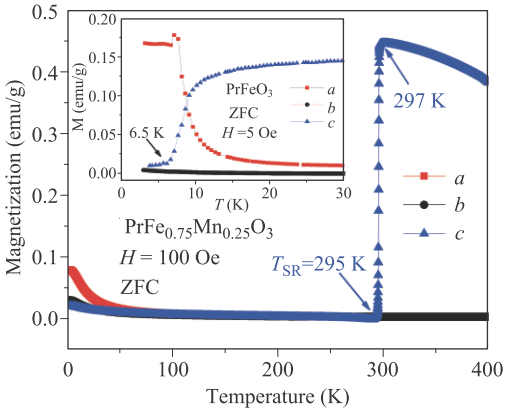

Fig. 4 Zero-filed-cooled (ZFC) curves of $PrFe_{0.75}Mn_{0.25}O_3$ single crystal along a-axis, b-axis and c-axis under the external magnetic field of 100 Oe. The inset is the ZFC curves of $PrFeO_3$ along the a, b and c axes under the external magnetic field of 5 Oe.

inset of Fig. 4 shows the magnetization measurement results of the parent $PrFeO_3$ sample for comparison. From the ZFC curves in Fig. 4, we noticed that the moments along the a and b axes are negligible in the whole temperature range of measurement from 2 K to 400 K whereas the magnetization along the c-axis displays a sharp jump from 0.45 emu/g to 0 as the temperature decreases from 297 K to 295 K. The weak ferromagnetic moment of the $PrFe_{0.75}Mn_{0.25}O_3$ sample falls to absolute zero when the temperature is below 295 K. Such a phase transition is identified to be from the Γ_4 phase with a weak magnetization along the c axis to the Γ_1 phase with a collinear antiferromagnetic structure upon cooling across the transition temperature. This Γ_4–Γ_1 SR transition is dramatically different from the Γ_4–Γ_2 phase transition of the parent $PrFeO_3$ material as depicted in Fig. 4 (inset), where the net magnetization changes from the c axis to a axis across the transition temperature upon cooling. In addition to the modification of the SR transition type, we also note that the doping of Mn pushes the SR transition temperature to around room temperature which is almost 300 K higher than that of the parent $PrFeO_3$ single crystal. Such a huge improvement in the SR transition temperature has never been reported elsewhere in rare-earth iron oxides [27, 28, 31–33]. When the temperature is higher than 297 K, Fe^{3+} begins to appear in magnetic order, and the interaction between Fe^{3+}–Fe^{3+} is much stronger than the interaction between Pr^{3+}–Fe^{3+} and Pr^{3+}–Pr^{3+}, occupying a dominant position. At this time, the system is in the Γ_4 state. With the decrease of temperature, the interaction between Pr^{3+}–Fe^{3+} gradually increases. Under the action of symmetry and antisymmetry, the Γ_4 spin structure in the system becomes extremely unstable. With the further strengthening of the interaction between Pr^{3+}–Fe^{3+}, the system underwent a spin orientation phase transition. Since the incorporation of Mn^{3+} replaces the position of Fe^{3+} in the system, and Mn^{3+} has a large magnetic anisotropy, when the temperature is lower than 295 K, the interaction of Fe^{3+}–Fe^{3+} and the interaction of Fe^{3+}/Mn^{3+}–Pr^{3+} jointly cause the system to be in the Γ_1 phase, which has also been observed in $TbFe_{1-x}Mn_xO_3$ [34]. With the increase of Mn ion concentration, the spin reorientation phase transition temperature move towards the high temperature direction, as shown in Fig. 3. The transition temperature of the doped $PrFeO_3$ is related to the anisotropy fields that is dependent on the Mn concentration. The formalism "$T(x) = \frac{1}{\kappa'}\log(\frac{x}{x_c})$" (where κ' is a positive constant related to the second-order anisotropic field and x_c represents a critical doping concentration) developed by Holmes [35] well describes the Mn doping dependence of the spin-reorientation temperatures of our grown samples with Mn doping from 0.1 to 0.3. In addition, the magnetization along the three directions has a significant increase at low temperatures, which is due to the ordering of Pr^{3+} rare earth ion at low temperatures.

In order to get a clearer insight into the magnetic behavior of $PrFe_{0.75}Mn_{0.25}O_3$ single crystal, we performed M–H measurement along the c-axis as well as along the a-axis at different temperatures. We chose four different temperatures including 50 K, 250 K that are below the SR transition temperature and 300 K, 350 K that are above the SR phase transition temperature. As shown in Fig. 5, we observe straight lines of M–H curves along both the c axis and a axis measured at 50 K and 250 K, which indicates a collinear antiferromagnetic structure described by Γ_1 where the spins of the rare-earth ions and transition-metal ions are aligned anti-parallel to each other and a

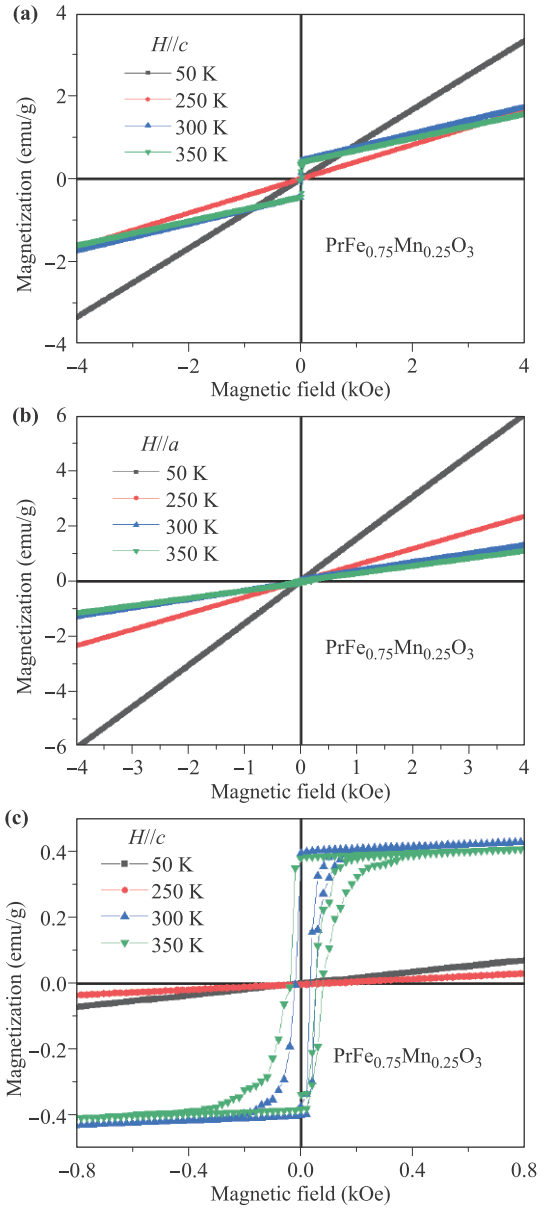

Fig. 5 Magnetization curves of $PrFe_{0.75}Mn_{0.25}O_3$ single crystal at different temperatures along the **(a)** c-axis and **(b)** a-axis; **(c)** is an enlarged version of Fig. 5(a) for the small field.

ferromagnetic component is forbidden. In contrast, magnetic hysteresis is observed at 300 K and 350 K along the c axis, indicative of a weak ferromagnetic component arising from a canted antiferromagnetic structure described by Γ_4 with antiferromagnetically coupled spins along the a axis and an allowed net magnetization along the c axis. The M–H measurement therefore further confirms the Γ_4 to Γ_1 SR transition of the grown Mn-doped $PrFeO_3$ single crystals, consistent with the M–T measurement in Fig. 4. It should be noted that the Γ_4 to Γ_1 spin reorientation transition reported here is considerably less investigated and rarely reported compared to the Γ_4 to Γ_2 transition which is the case for the parent $PrFeO_3$ and many other orthoferrites.

The study of the magnetic phase transition of $PrFeO_3$ single crystal under different magnetic fields shows that the $PrFeO_3$ sample is very sensitive to the change of the magnetic field [26]. In order to study the influence of the magnetic field on the Γ_4–Γ_1 transition temperature of the Mn-doped $PrFeO_3$, we carried out the magnetization measurements of $PrFe_{0.75}Mn_{0.25}O_3$ single crystal under different magnetic fields. Since there is negligible magnetization along the a-axis and b-axis in the whole temperature range of measurement, we only present the M–T curves along the c-axis here. It can be seen from Fig. 6 that the SR transition temperature remains almost the same in a wide range of magnetic fields from 10 Oe to 10000 Oe. In addition, the process of the Γ_4–Γ_1 SR transition completes within an interval of 2 K. Based on the combined numerous features they possess: the capability of modulating the SR transition temperature in a wide range of temperatures including room temperature, the robustness of the SR transition temperature against perturbation of magnetic fields, together with a narrow SR transition interval of 2 K, the Mn-doped $PrFeO_3$ single crystals are expected to be a temperature sensitive material device for thermo-controlled magnetic switching. It should be noted that these findings further prove that the doping of manganese enriches the interaction between rare earth ions, iron ions and manganese ions, and has a significant impact on the magnetic properties of the system.

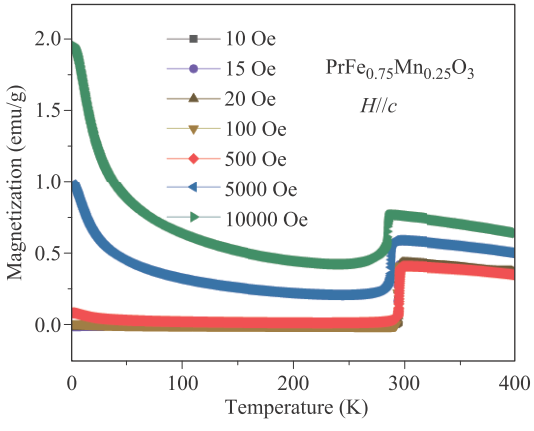

Fig. 6 M–T curves of $PrFe_{0.75}Mn_{0.25}O_3$ single crystal along c-axis under different applied magnetic fields.

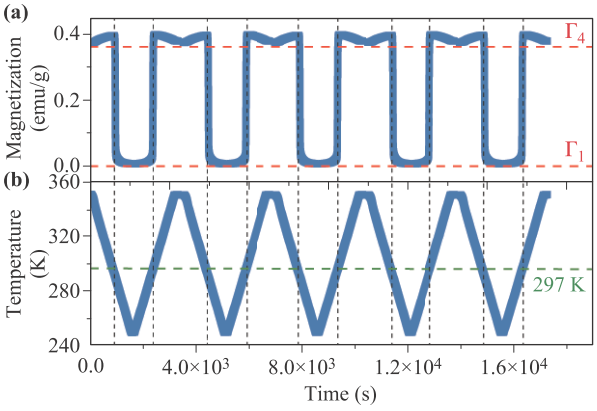

Fig. 7 **(a)** The magnetization versus time curve of $PrFe_{1-x}Mn_xO_3$ ($x = 0.25$) single crystal along the c axis. **(b)** The temperature vs. time curve of $PrFe_{1-x}Mn_xO_3$ ($x = 0.25$) single crystal along the c axis.

As a new type of magnetic thermo-sensitive material, spin reorientation phase transition material may be used in magnetic thermo-sensitive devices to enrich the application range of such devices. But to be able to apply, in addition to the spin reorientation temperature at room temperature, the material also needs to be magnetically stable, able to withstand repeated magnetization and demagnetization. So we did the experiment in Fig. 7. Repeated heating and cooling tests were carried out in the c axis of $PrFe_{1-x}Mn_xO_3$ ($x = 0.25$) single crystal with a temperature range of 250–350 K. The magnetization intensity and temperature were respectively charted with time, and it was found that the heating and cooling curves of each repetition could completely coincide with the previous one. The dotted green line in Fig. 6 corresponds to a transition temperature of 297 K. The sample belongs to Γ_4 phase above 297 K, but quickly changes to Γ_1 phase below 297 K. The above measurements in the temperature range near the phase transition repeatedly raised and dropped, it was found that in this process, the change path of the magnetization value was almost the same every time, which has a good repeatability and stability, so it can be used as the material for magnetic thermal sensing devices.

4 Conclusion

In summary, we have successfully fabricated a series of Mn-doped $PrFe_{1-x}Mn_xO_3$ (where $x = 0$, 0.1, 0.2, 0.25, 0.3) single crystals by optical floating zone method. The SR phase transitions from Γ_4 to Γ_1 have been observed in all the Mn-doped $PrFeO_3$ single crystals and confirmed by magnetization measurement along different crystal axes. Interestingly, the SR phase transition of the Mn-doped $PrFeO_3$ is dramatically different from the SR transition

from Γ_4 to Γ_2 of the parent $PrFeO_3$ compound without doping. The transition temperature can be modulated from 196 K towards 317 K by different Mn doping. Remarkably, $PrFe_{1-x}Mn_xO_3$ with thermo-controlled magnetic switching effect is expected to be a new type of temperature sensitive material. The origin of the modification of the SR transition type and transition temperature in Mn-doped $PrFeO_3$ remains unknown which requires future investigation using neutron scattering. One possible origin is the competing coupling between Pr–Fe and Pr–Mn exchange interaction. This demonstrated control scheme of spin reorientation transition temperature by Mn substitution of Fe on the transition-metal site is expected to be applicable to many other rare-earth orthoferrites and can be used as device materials for thermal controllable magnetic switching.

Acknowledgements This work was supported by the Ministry of Science and Technology of the People's Republic of China (No. 2018YFB0704402), the National Natural Science Foundation of China (NSFC, Nos. 12074242, 11774217, and 12074241), and the Science and Technology Commission of Shanghai Municipality (No. 21JC1402600).

References

1. V. Skumryev, S. Stoyanov, Y. Zhang, G. Hadjipanayis, D. Givord, and J. Nogués, Beating the superparamagnetic limit with exchange bias, *Nature* 423(6942), 850 (2003)
2. I. Fita, A. Wisniewski, R. Puzniak, E. E. Zubov, V. Markovich, and G. Gorodetsky, Common exchange-biased spin switching mechanism in orthoferrites, *Phys. Rev. B* 98(9), 094421 (2018)
3. A. V. Kimel, A. Kirilyuk, A. Tsvetkov, R. V. Pisarev, and Th. Rasing, Laser-induced ultrafast spin reorientation in the antiferromagnet $TmFeO_3$, *Nature* 429(6994), 850 (2004)
4. Y. Yang, R. B. Wilson, J. Gorchon, C. H. Lambert, S. Salahuddin, and J. Bokor, Ultrafast magnetization reversal by picosecond electrical pulses, *Sci. Adv.* 3(11), e1603117 (2017)
5. Th. Gerrits, H. A. M. van den Berg, J. Hohlfeld, L. Bär, and Th. Rasing, Ultrafast precessional magnetization reversal by picosecond magnetic field pulse shaping, *Nature* 418(6897), 509 (2002)
6. H. W. Schumacher, C. Chappert, R. C. Sousa, P. P. Freitas, and J. Miltat, Quasiballistic magnetization reversal, *Phys. Rev. Lett.* 90(1), 017204 (2003)
7. W. C. Koehler, E. O. Wollan, and M. K. Wilkinson, Neutron diffraction study of the magnetic properties of rare-earth-iron perovskites, *Phys. Rev.* 118(1), 58 (1960)
8. A. V. Kimel, B. A. Ivanov, R. V. Pisarev, P. A. Usachev, A. Kirilyuk, and Th. Rasing, Inertia-driven spin switching in antiferromagnets, *Nat. Phys.* 5(10), 727 (2009)
9. D. Treves, Magnetic studies of some orthoferrites, *Phys. Rev.* 125(6), 1843 (1962)
10. R. L. White, Review of recent work on the magnetic and spectroscopic properties of the rare-earth orthoferrites, *J. Appl. Phys.* 40(3), 1061 (1969)
11. S. Cao, H. Zhao, B. Kang, J. Zhang, and W. Ren, Temperature induced spin switching in $SmFeO_3$ single crystal, *Sci. Rep.* 4(1), 5960 (2015)
12. J. Guo, L. Cheng, Z. Ren, W. Zhang, X. Lin, Z. Jin, S. Cao, Z. Sheng, and G. Ma, Magnetic field tuning of spin resonance in $TmFeO_3$ single crystal probed with THz transient, *J. Phys.: Condens. Matter* 32(18), 185401 (2020)
13. M. Shao, S. Cao, Y. Wang, S. Yuan, B. Kang, J. Zhang, A. Wu, and J. Xu, Single crystal growth, magnetic properties and Schottky anomaly of $HoFeO_3$ orthoferrite, *J. Cryst. Growth* 318(1), 947 (2011)
14. J. C. Walling and R. L. White, Study of magnetic interactions in $HoFeO_3$, *Phys. Rev. B* 10(11), 4748 (1974)
15. D. Afanasiev, B. A. Ivanov, A. Kirilyuk, Th. Rasing, R. V. Pisarev, and A. V. Kimel, Control of the ultrafast photo-induced magnetization across the Morin transition in $DyFeO_3$, *Phys. Rev. Lett.* 116(9), 097401 (2016)
16. G. Zhao, W. Fan, H. Chen, X. Ma, B. Kang, W. Lu, J. Zhang, and S. Cao, $4f$–$3d$ interaction dominated field tailoring spin switching in rare earth doped $Dy_{0.5}Er_{0.5}FeO_3$ single crystal, *Appl. Mater. Today* 23, 101070 (2021)
17. X. Luo, R. Li, X. Ma, Y. Chen, B. Kang, J. Zhang, W. Ren, Z. Feng, and S. Cao, Doping tuned spin reorientation and spin switching in praseodymium–samarium orthoferrite single crystals, *J. Phys.: Condens. Matter* 33(27), 275803 (2021)
18. M. H. Mohammed, J. Horvat, Z. Cheng, S. Cao, E. Li, and R. Li, Magnetic interaction between Pr^{3+} and Dy^{3+} spins and their spin transition induced by magnetic field in a $Dy_{0.5}Pr_{0.5}FeO_3$ single crystal, *J. Phys. Chem. C* 123(50), 30584 (2019)
19. G. Wang, W. Zhao, Y. Cao, B. Kang, J. Zhang, W. Ren, and S. Cao, Temperature-induced spin reorientation and magnetization jump of rare-earth orthoferrite $Ho_{0.5}Pr_{0.5}FeO_3$ single crystal, *J. Alloys Compd.* 674, 300 (2016)
20. X. Luo, X. Ma, Y. Chen, B. Kang, W. Lu, Z. Feng, J. Y. Ge, J. Zhang, and S. Cao, Doping induced very low field type II spin switching in single crystal $Nd_{0.7}Sm_{0.3}FeO_3$, *Ceram. Int.* 46(11), 17347 (2020)
21. X. Ma, N. Yuan, X. Luo, Y. Chen, B. Kang, W. Ren, J. Zhang, and S. Cao, Field tunable spin switching in perovskite $YbFeO_3$ single crystal, *Mater. Today Commun.* 27, 102438 (2021)
22. N. Yuan, R. B. Li, Y. S. Yu, Z. J. Feng, B. J. Kang, S. Y. Zhuo, J. Y. Ge, J. C. Zhang, and S. X. Cao, Tuning spin reorientation in $Er_{1-x}Y_xFeO_3$ single crystal family, *Front. Phys.* 14(1), 13502 (2019)
23. Q. Zhang, W. Tian, S. G. Peterson, K. W. Dennis, and D. Vaknin, Spin reorientation and Ce–Mn coupling in antiferromagnetic oxypnictide CeMnAsO, *Phys. Rev. B* 91(6), 064418 (2015)

24. A. M. Vibhakar, D. D. Khalyavin, P. Manuel, L. Zhang, K. Yamaura, P. G. Radaelli, A. A. Belik, and R. D. Johnson, Magnetic structure and spin-flop transition in the *A*-site columnar-ordered quadruple perovskite $TmMn_3O_6$, *Phys. Rev. B* 99(10), 104424 (2019)
25. M. Abdellahi, A. S. Abhari, and M. Bahmanpour, Preparation and characterization of orthoferrite $PrFeO_3$ nanoceramic, *Ceram. Int.* 42(4), 4637 (2016)
26. E. Li, Z. Feng, B. Kang, J. Zhang, W. Ren, and S. Cao, Spin switching in single crystal $PrFeO_3$ and spin configuration diagram of rare earth orthoferrites, *J. Alloys Compd.* 811, 152043 (2019)
27. H. Shen, Z. Cheng, F. Hong, J. Xu, X. Wang, J. Wang, Z. Yu, and Y. Wang, Structure, room temperature spin reorientation and its dynamics in $DyFe_{0.6}Mn_{0.4}O_3$, *J. Alloys Compd.* 680, 226 (2016)
28. F. Hong, Z. Cheng, H. Zhao, H. Kimura, and X. Wang, Continuously tunable magnetic phase transitions in the $DyMn_{1-x}Fe_xO_3$ system, *Appl. Phys. Lett.* 99(9), 092502 (2011)
29. J. Kang, Y. Yang, X. Qian, K. Xu, X. Cui, Y. Fang, V. Chandragiri, B. Kang, B. Chen, A. Stroppa, S. Cao, J. Zhang, and W. Ren, Spin-reorientation magnetic transitions in Mn-doped $SmFeO_3$, *IUCrJ* 4(5), 598 (2017)
30. M. Mihalik, Z. Jagličić, M. Fitta, V. Kavečanský, K. Csach, A. Budziak, J. Briančin, M. Zentková, and M. Mihalik, Structural and magnetic study of $PrMn_{1-x}Fe_xO_3$ compounds, *J. Alloys Compd.* 687, 652 (2016)
31. Y. Nagata, S. Yashiro, T. Mitsuhashi, A. Koriyama, Y. Kawashima, and H. Samata, Magnetic properties of $RFe_{1-x}Mn_xO_3$ (R = Pr, Gd, Dy), *J. Magn. Magn. Mater.* 237(3), 250 (2001)
32. B. Deka, S. Ravi, A. Perumal, and D. Pamu, Effect of Mn doping on magnetic and dielectric properties of $YFeO_3$, *Ceram. Int.* 43(1), 1323 (2017)
33. Y. H. Huang, M. Karppinen, N. Imamura, H. Yamauchi, and J. B. Goodenough, Structural transformation and magnetic competition in $Yb(Mn_{1-x}Fe_x)O_3$, *Phys. Rev. B* 76(17), 174405 (2007)
34. Y. Cao, M. Xiang, W. Zhao, G. Wang, Z. Feng, B. Kang, A. Stroppa, J. Zhang, W. Ren, and S. Cao, Magnetic phase transition and giant anisotropic magnetic entropy change in $TbFeO_3$ single crystal, *J. Appl. Phys.* 119(6), 063904 (2016)
35. L. Holmes, L. G. Van Uitert, and R. Hecker, Effect of Co on magnetic properties of $ErFeO_3$, $HoFeO_3$, and $DyFeO_3$, *J. Appl. Phys.* 42(2), 657 (1971)